Eur Biophys J (2008) 37:1077–1082
DOI 10.1007/s00249-008-0327-7

BIOPHYSICS LETTER

The hand of the filamentous bacteriophage helix

S. K. Straus · W. R. P. Scott · D. A. Marvin

Received: 21 January 2008 / Revised: 27 March 2008 / Accepted: 2 April 2008 / Published online: 18 April 2008

Abstract Filamentous bacteriophage (*Inovirus*) is a widely studied model system in molecular biophysics. The structure of the virion has been analysed by various methods, but the methods have seldom questioned the hand of the virion helix. The hand of the helix relating the protein subunits in the class II virus strain Pf1 was chosen by calculating an electron-density distribution from X-ray fibre diffraction data, using a maximum-entropy method, but to our knowledge this method has not been used for a similar purpose in any other system. Moreover, this same hand was extended only by analogy, with no direct analysis of the corresponding data, to the class I virus strain Ff (fd, f1, M13), which has a different helix symmetry. Here we use published solid-state NMR data to confirm the validity of the hand of Pf1 chosen by the maximum-entropy method, and to confirm the extension to Ff.

Keywords α-Helix · Fibre diffraction · Solid-state NMR

Abbreviations

PDB	Protein Data Bank
PISA	Polarity index slant angle
PISEMA	Polarisation inversion spin exchange at the magic angle
rmsd	Root-mean-square deviation

S. K. Straus · W. R. P. Scott
Department of Chemistry,
University of British Columbia,
V6T 1Z1 BC, Canada

D. A. Marvin (✉)
Department of Biochemistry,
University of Cambridge,
Cambridge CB2 1GA, UK
e-mail: d.a.marvin@bioc.cam.ac.uk

Introduction

Filamentous bacteriophage is a simple and widely used system in molecular biophysics (reviewed by Hansen et al. 2000; Webster 2001; Russel and Model 2006; Khalil et al. 2007). The virion is an elongated particle about 60 Å in diameter and 1–2 μm long, depending on the biological strain. Most of the virion capsid is a roughly cylindrical shell formed by several thousand ~50-residue identical α-helical subunits in an overlapping interdigitated helical array, protecting a single-stranded circular DNA core. A few minor proteins cap the two ends of the virion. Two symmetry classes of filamentous phage have been identified by X-ray fibre diffraction: class I, typified by the Ff (fd, f1, M13) strain; and class II, typified by the Pf1 strain (Fig. 1). Early models of the Pf1 virion (Marvin and Wachtel 1976; Makowski et al. 1980) assumed that the crossing angle between adjacent subunits in the virion would be the same as for the coiled-coil model of α-helix (Crick 1953), and this predicts a left-handed sense for the helix of subunits in the class II virion (Fig. 1d). But the electron-density distribution calculated from native and single-isomorphous derivative data using a maximum-entropy method (Bryan et al. 1983; Bryan 1987; Marvin et al. 1987) showed that if the left-handed sense for the helix of subunits is used, the α-helix of the subunit itself appears to be left-handed, contrary to fact. The implication of this result is that the arrangement of class II helix subunits is in fact right-handed, Fig. 1b. The maximum-entropy method gave an interpretable model-independent electron density map, enabling refinement of models with respect to the quantitative X-ray data (Gonzalez et al. 1995). The different symmetry of the class I virions means that measurable diffraction data for class I diffraction patterns are much less extensive, because many of the

Bessel function terms are superimposed. The corresponding data distributions cannot be resolved, and the maximum-entropy method is not applicable. Molecular models of class I took the right-handed sense, Fig. 1a, from the Pf1 class II symmetry by analogy, with no further experimental data. Tombolato et al. (2006) demonstrated that in the liquid crystalline phase of Ff, 'left-handed supramolecular helicity is observed, whereas right handedness would be expected for purely steric reasons'. These findings are based on the observation of left-handedness from fluorescence microscopy and supported by the argument that electrostatic interactions drive this arrangement. Given these uncertainties, the hand of the virion helix is worth further direct investigation.

Solid-state NMR studies of aligned filamentous phage can give important structural information. Analysis of these data has until now implicitly assumed the validity of the maximum-entropy choice of hand for Pf1, and the extension by analogy to fd. Here we show that the methods developed to determine the orientation of α-helices in lipid bilayers using solid-state NMR can also be applied to determine the hand of the filamentous bacteriophage virion, confirming that the hand determined by the maximum-entropy method is correct. Although this conclusion is implicit in the published solid-state NMR data, it has not previously been explicitly discussed. Our results show that all three types of data (X-ray fibre diffraction, molecular model-building, and solid-state NMR) are necessary to unambiguously solve the structures of filamentous bacteriophage.

Materials and methods

To illustrate the difference between left- and right-handed models of filamentous phage (Fig. 1), equivalent points in the protein subunits of a helical capsid are projected along radii onto a cylindrical surface concentric with the helix axis; the cylinder is then cut vertically, opened flat and viewed from the outside. The broken line represents the axis of the α-helix associated with an arbitrary subunit with index 0; identical subunits (not shown) are associated with all other surface lattice points. The indices of subunits nearest to subunit 0 are shown. The horizontal dimension of this radial projection corresponds to a cylinder of radius about 8 Å; for larger radii the angle between the subunit axis and the virion axis would appear larger in the radial projection. The solid line follows the basic helix, which for Pf1 is the helix with the smallest increase in z from one subunit to the next. For Pf1 in the higher-temperature symmetry shown, there are 5.40 subunits per turn in a simple helix of pitch 15.66 Å. A 'basic helix' with a pitch of 16.15 Å is also drawn for fd to indicate the similarity

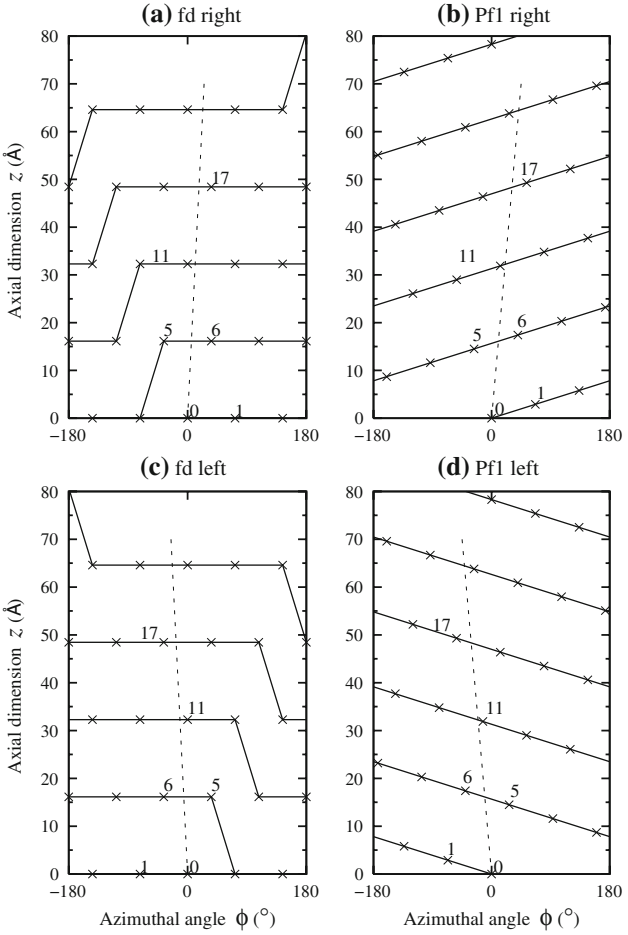

Fig. 1 Surface lattices (radial projections) of filamentous bacteriophage capsids in the class I and class II symmetries, typified by the fd and Pf1 strains, respectively. Equivalent points (x) in the protein subunits of a helical capsid are projected along radii onto a cylindrical surface concentric with the helix axis; the cylinder is then cut vertically, opened flat and viewed from the outside. The indices of subunits nearest to an arbitrary subunit with index 0 are shown. The *broken lines* represent the axis of the α-helix associated with subunit 0; identical *parallel lines* (not shown) are associated with all other surface lattice points. The two surface lattices **a** and **b** show the right-handed forms of the fd and Pf1 lattices, respectively; lattices **c** and **d** show the corresponding left-handed forms (see Marvin et al. 1994, 2006 for further discussion)

between the two assemblages. For fd in the dyad symmetry shown, there are five subunits at any one z height, related by a fivefold rotation axis. Successive rings of five subunits are related by a twofold screw axis along the helix, with a 32.3 Å repeat.

To build molecular models of the low-resolution enantiomorph, we mirror a right-handed model of a subunit, shown schematically in Fig. 1a and b, across the $x = 0$ plane using MOLEMAN2 (Kleywegt 1997). This mirror image will be a true enantiomorph, so both the isomers of the amino-acid residues and the sense of the α-helix will be incorrect (i.e. D-amino acid residues and a left-handed

α-helix). We then fit the correct molecular model of the subunit structure to this enantiomorph, using the option 'fit selected residues' for all backbone atoms in the Swiss-PDB viewer (Guex and Peitsch 1997), to give a structurally correct α-helix subunit that forms a virion with the opposite hand, shown schematically in Fig. 1c and d. We confirm by inspection that the subunit in the new orientation packs well with nearest neighbours, with the acidic groups exposed on the outside of the virion, basic residues pointing inward to neutralize the DNA charge at the core of the virion, and apolar groups involved in interactions between neighbouring subunits, and is consistent with other non-diffraction data (Marvin et al. 1994; Gonzalez et al. 1995; Welsh et al. 2000; Marvin et al. 2006).

We calculate the molecular transform of fd models to compare with X-ray fibre diffraction data as described previously, including corrections for the DNA core and for the solvent surrounding the virion (Marvin et al. 1987; Gonzalez et al. 1995; Welsh et al. 2000; Marvin et al. 2006). The solvent-corrected amplitudes $[\Sigma_n|F_{n,l}(R)|^2]^{1/2}$ calculated for the model are compared with the observed diffraction amplitudes $I_l(R)^{1/2}$. For $l = 0$, the $J_0(R)$ transform of a DNA model is added to the $J_0(R)$ transform of the protein model.

The ^{15}N chemical shift/^{15}N–^{1}H dipolar correlation solid state NMR data (PISEMA spectrum) of an amino acid can be used to define the orientation with respect to the magnetic field for both the NH vector and the normal to the peptide plane. Thus the PISEMA spectrum of an α-helix gives an array of points, the polarity index slant angle (PISA) wheel, which can define both the tilt of the α-helix with respect to the magnetic field (slant angle) and the rotation of the tilted α-helix about its own axis (polarity index) (Marassi and Opella 2000, 2002, 2003; Wang et al. 2000; Denny et al. 2001). Equivalent points in all amino acid residues of an α-helix projected down the helix axis form a circular array (sometimes called the 'helical wheel'), and the PISA wheel can be mapped into this axial projection. This mapping is especially clear when the axis of the α-helix is tilted by a relatively small angle (about 20°–40°) with respect to the direction of the magnetic field. Labelling of specific amino acids with ^{15}N can enable determination of the rotation of the tilted α-helix about its own axis, the polarity index, because labelling of a specific amino acid that is asymmetrically distributed in the amino acid sequence will be mapped into an asymmetric distribution on the PISA wheel (Marassi and Opella 2000, 2002, 2003; Wang et al. 2000; Denny et al. 2001).

For fd, the molecular model that we use is PDB entry 2C0X, which is PDB entry 1IFJ (Marvin et al. 1994) that has been refined (Marvin et al. 2006) with respect to both X-ray fibre diffraction data and the NMR PISEMA data of Zeri et al. (2003). To explore further the possible structural validity of the left-handed symmetry, we refine the left-handed structure derived from 2C0X (which we call model 2C0X-left) using the program FX-PLOR (Wang and Stubbs 1993) as described by Marvin et al. (2006) for model 2C0X. We refine model 2C0X-left with respect to both molecular energy and fit to X-ray data, while maintaining a large harmonic restraint on the coordinates of backbone atoms, to maintain the backbone structure and therefore the calculated PISEMA values. Initially the energy of non-bonded contacts between sidechains of symmetry-related nearest neighbours is very high, but this is quickly reduced by refinement, and the fit to the X-ray data is maintained ($R = 0.20$), to give model 2C0X-left-ref3. To examine the environment of each subunit, we generate the coordinates of the ten non-bonded symmetry-related subunits surrounding an arbitrary subunit, as discussed by Marvin et al. (1994). We use the program ANOLEA (Melo and Feytmans 1998) to calculate for this arbitrary subunit (and therefore for every identical subunit) a non-local energy profile, that includes both the van der Waals interactions between non-bonded atoms, and the accessible atomic surface.

For Pf1, the choice of model is more complicated. The helix symmetry of the Pf1 virion changes reversibly between two slightly different forms at about 283 K. Refinement of the higher-temperature form with respect to X-ray data led to the suggestion that the true asymmetric unit was best represented as a 'group of three' polypeptide chains having slightly different orientations, PDB entry 1QL2, rather than a single polypeptide chain, PDB entry 1QL1 (Welsh et al. 2000). Challenges to this suggestion based on solid-state NMR data from aligned samples (Thiriot et al. 2004) and magic-angle spinning NMR data (Goldbourt et al. 2007) used the deposited coordinates for the 'group of three' polypeptide chains, PDB entry 1QL2, in which there are slight differences not only in the orientations of the three subunits, but also in their conformation (because of the refinement method). But Welsh et al. (2000) also reported that if the subunits in the 'group of three' are replaced by subunits with identical conformation but still with slightly different orientations, the model still explains the X-ray data (Fig. 5c of Welsh et al. 2000). The technique used by Goldbourt et al. (2007) would not detect differences in orientation of identical subunits, so their challenge does not apply. The differences in the PISEMA spectrum identified by Thiriot et al. (2004) result mainly from the small differences in subunit structure, which disappear when the model of Fig. 5c of Welsh et al. (2000) is used (our unpublished calculations). Therefore the 'group of three' model is not ruled out. But for the present discussion, we refine the single subunit model PDB entry 1QL1 (Welsh et al. 2000) to fit not only the X-ray data but also the NMR PISEMA data of Thiriot

et al. (2004), using Xplor-NIH (Schwieters et al. 2003, 2006). Our refinement approach for Pf1 is similar to that used for fd model 2C0X (Marvin et al. 2006). The rmsd for all backbone atoms in residues 7–45 is 1.2 Å between Pf1 model 1QL1 and our refined model n18 (in preparation), and this difference does not affect our calculations of hand.

To compare observed and calculated PISEMA values, we calculate an approximate centre of mass (Wang et al. 2000) of the calculated PISEMA spectrum of all α-helix residues in the right-handed model, from residues 7 to 49 (for fd model 2C0X) or 7 to 45 (for Pf1 model n18). We then draw vectors (arrows) from this centre to the PISEMA values calculated for the residues with the indices shown (i.e. the labelled residues). We plot the corresponding observed PISEMA values for these labelled residues. If the hand of the calculated model is correct, there will be calculated vectors that roughly match all the observed labelled PISEMA values (Wang et al. 2000). If calculated vectors are far from any corresponding observed values, the polarity index of the α-helix, and therefore the orientation of the subunit in the model, cannot be correct.

Results and discussion

For the left-handed fd model, 2C0X-left, the initial structure shows very bad sidechain contact energy, but brief refinement of sidechain energy, while keeping the backbone structure (and therefore the NMR calculations) unchanged yields a model (2C0X-leftref3) with generally good stereochemistry and a good fit to the X-ray data. The X-ray fibre diffraction pattern calculated for subunit 2C0X in the right-handed symmetry of fd (Fig. 2a) fits the observed data little better than the pattern calculated for the same subunit refined in the left-handed symmetry, model 2C0X-leftref3 (Fig. 2b). Both these calculated patterns fit the observed data better than the pattern calculated for model 1NH4 derived from solid-state NMR data by Zeri et al. (2003) in the right-handed symmetry (Fig. 3b of Marvin et al. 2006). These calculations show that it is difficult to choose between left- and right-handed models of fd from the fit to native X-ray fibre diffraction data alone.

The non-local energy profile, defined by contacts between symmetry-related neighbouring subunits and the distribution of buried and accessible residues in the assembly (Melo and Feytmans 1998), is acceptable for the right-handed fd model 2C0X, as expected (Fig. 3). In the non-local energy profile of the refined left-handed model, 2C0X-leftref3, there are only a few poor regions (Fig. 3), and it would be difficult to use this energy profile to rule out left-handed models. Residues Gly34, Ala35 and Gly38 are poor because of accessibility problems, not close

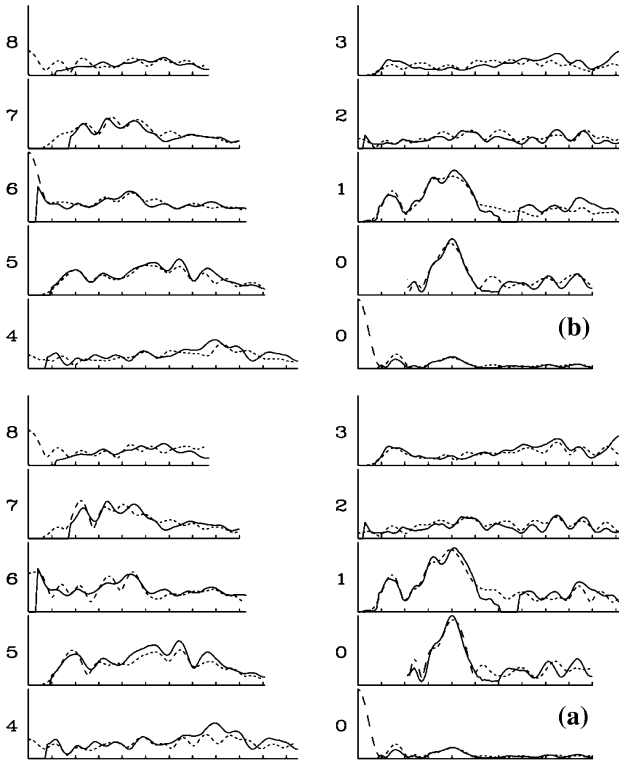

Fig. 2 Calculated continuous transforms of fd models in the dyad symmetry, broken curves, compared with the observed diffraction data of Marvin et al. (2006), *solid curves*. The number at the left of each curve is the *layer line* index l for the helix repeat $c = 32.3$ Å. The horizontal axis is $R = 2\sin\theta/\lambda$ Å^{-1} where θ is the diffraction angle and λ is the X-ray wavelength 1.488 Å. Scale divisions start at $R = 0.0$ Å^{-1} at the left-hand side, and are at intervals of $R = 0.025$ Å^{-1}. The lower plot of $l = 0$ is on a reduced scale, to display the strong inner region of $l = 0$. **a** Calculated transform of fd model 2C0X in the right-handed symmetry of Fig. 1a (identical to Fig. 3a of Marvin et al. 2006). **b** Calculated transform of fd model 2C0X-leftref3, which is the same subunit structure but refined in the left-handed symmetry of Fig. 1c

contacts; and inspection of the model suggests that close contacts at Trp26 and Phe42 can be easily repaired by slight shifts in the subunit backbone. This model was derived by simple energy minimization, and further exhaustive refinement involving rebuilding of poor regions and simulated-annealing refinement should yield a left-handed model that is fully consistent with the X-ray and stereochemical data. We have also calculated the non-local energy profile of model 1NH4 (Zeri et al. 2003); it is far worse than that of model 2C0X-leftref3, presumably because non-local contacts were not refined for model 1NH4.

Testing models using specifically labelled PISEMA data is illustrated for fd in Fig. 4 with the NMR data of Zeri et al. (2003). The calculated vectors for Leu residues 14 and 41 point towards observed Leu residues (*) in model 2C0X (Fig. 4a), but not (especially residue 41) in model 2C0X-left (Fig. 4c). For model 2C0X-left, the calculated

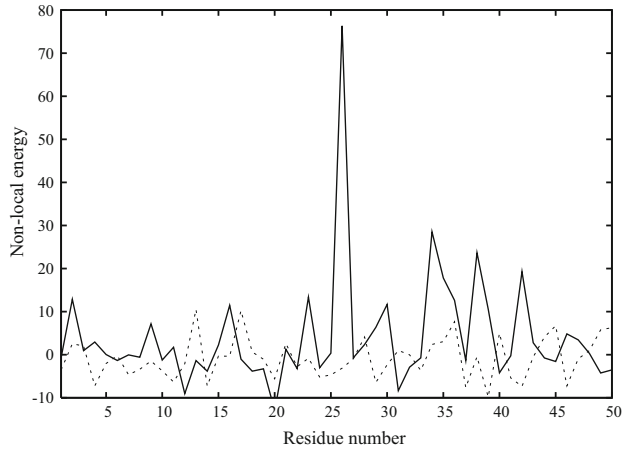

Fig. 3 Non-local energy profile scores for fd models. *Solid curve*, left-handed model 2C0X-leftref3. *Broken curve*, right-handed model 2C0X (Marvin et al. 2006)

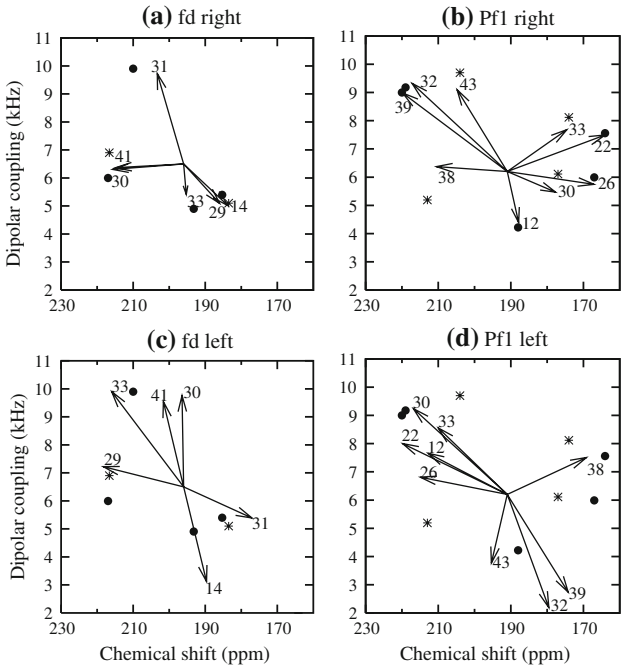

Fig. 4 Observed two-dimensional PISEMA spectra of filamentous bacteriophage, compared with the calculated spectra from molecular models in the right- and left-handed symmetries. **a** fd in the right-handed symmetry; **b** Pf1 in the right-handed symmetry; **c** fd in the left-handed symmetry **d** Pf1 in the left-handed symmetry. The observed fd spectrum, from Zeri et al. (2003), is shown for ^{15}N-specifically labelled amino acid residues Leu (residues 14, 41, represented by *) and Val (residues 29, 30, 31, 33, represented by •). The observed Pf1 spectrum, from Thiriot et al. (2004), is shown for ^{15}N-specifically labelled amino acid residues Leu (residues 30, 33, 38, 43, represented by *) and Ile (residues 12, 22, 26, 32, 39, represented by •). For both fd and Pf1 models, the calculated PISEMA values are shown as vectors from a centre determined from the calculated right-handed PISEMA distribution (see text)

vectors for both Val 30 and 33 point towards only a single observed labelled Val (•), whereas there is only a single calculated Val vector (Val31) pointing towards two observed labelled Val; for model 2C0X, the observed and calculated values match.

Similar calculations for Pf1, using the NMR data of Thiriot et al. (2004), confirm that the right-hand model is also correct for Pf1. The calculated vectors are near observed residues in the right-handed model (Fig. 4b). For the left-handed model, calculated vectors for Leu30 and Leu33 point towards a single observed Leu residue (*), whereas the single calculated vector for Leu38 points towards two observed Leu residues (Fig. 4d). For the left-handed model, the three calculated vectors for Ile12, Ile22 and Ile26 point towards only two observed Ile (•); the calculated vectors for Ile32 and Ile39 point towards a single observed labelled Ile; leaving no calculated Ile vectors pointing towards two observed labelled Ile. For the right-handed model, the observed and calculated values all roughly match. We conclude that for both fd and Pf1, the right-handed sense of the virion helix is correct, and the left-handed sense cannot be correct.

PISEMA data interpreted by PISA wheel analysis has been used to define the orientation of α-helices in membranes (Marassi and Opella 2003), and here we have shown that it can define the orientation of α-helices in virus coats. It may also be useful to determine structural details in other systems having α-helices aligned with respect to the magnetic field, as discussed by Marassi and Opella (2003).

Our proof that the subunits of both Pf1 and fd have a right-handed orientation in the virion, even though the symmetry relating the subunits is different for these two phages, is important to consideration of the detailed mechanism of assembly of filamentous bacteriophage.

There is another uncertainty about the Pf1 virion symmetry that was difficult to resolve using native X-ray fibre diffraction data and molecular model-building alone: are there 4.4 units per turn (Marvin and Wachtel 1976) or 5.4 units per turn (Makowski et al. 1980) in the 15.66 Å helix repeat? For these two options, local molecular contacts between adjacent subunits are almost identical, since the difference in the number of units per turn is counterbalanced by the difference in the axial rise per subunit; and the calculated transforms of the two types of model are also similar (Marvin et al. 1981). Intensity changes induced by a single isomorphous derivative indicate that the correct value is 5.4 units per turn, but it would be useful to address this question with a different experimental method.

Acknowledgments WRPS acknowledges support from the Canada Foundation for Innovation. SKS acknowledges support from the Natural Sciences and Engineering Research Council of Canada (University Faculty Award and Discovery Grant) and from the

University of British Columbia. DAM acknowledges support from the Department of Biochemistry, University of Cambridge.

References

Bryan RK (1987) Maximum entropy in structural molecular biology: the fiber diffraction phase problem. In: Smith CR, Erickson GJ (eds) Maximum-entropy and Baysian spectral analysis and estimation problems. Reidel, Dordrecht, pp 207–228

Bryan RK, Bansal M, Folkhard W, Nave C, Marvin DA (1983) Maximum-entropy calculation of the electron density at 4 Å resolution of Pf1 filamentous bacteriophage. Proc Natl Acad Sci USA 80:4728–4731

Crick FHC (1953) The packing of α-helices: simple coiled-coils. Acta Crystallogr 6:689–697

Denny JK, Wang J, Cross TA, Quine JR (2001) PISEMA powder patterns and PISA wheels. J Magn Reson 152:217–226

Goldbourt A, Gross BJ, Day LA, McDermott AE (2007) Filamentous phage studied by magic-angle spinning NMR: resonance assignment and secondary structure of the coat protein in Pf1. J Am Chem Soc 129:2338–2344

Gonzalez A, Nave C, Marvin DA (1995) Pf1 filamentous bacteriophage: Refinement of a molecular model by simulated annealing using 3.3Å resolution X-ray fibre diffraction data. Acta Crystallogr Sect D 51:792–804

Guex N, Peitsch MC (1997) Swiss-model and the Swiss-PDB viewer: an environment for comparative protein modeling. Electrophoresis 18:2714–2723

Hansen MR, Hanson P, Pardi A (2000) Filamentous bacteriophage for aligning RNA, DNA, and proteins for measurement of nuclear magnetic resonance dipolar coupling interactions. Methods Enzymol. 317:220–240

Khalil AS, Ferrer JM, Brau RR, Kottmann ST, Noren CJ, Lang MJ, Belcher AM (2007) Single M13 bacteriophage tethering and stretching. Proc Natl Acad Sci USA 104:4892–4897

Kleywegt GJ (1997) Validation of protein models from C^{α} coordinates alone. J Mol Biol 273:371–376

Makowski L, Caspar DLD, Marvin DA (1980) Filamentous bacteriophage Pf1 structure determined at 7 Å resolution by refinement of models for the α-helical subunit. J Mol Biol 140:149–181

Marassi FM, Opella SJ (2000) A solid-state NMR index of helical membrane protein structure and topology. J Magn Reson 144:150–155

Marassi FM, Opella SJ (2002) Using Pisa pies to resolve ambiguities in angular constraints from PISEMA spectra of aligned proteins. J Biomol NMR 23:239–242

Marassi FM, Opella SJ (2003) Simultaneous assignment and structure determination of a membrane protein from NMR orientational restraints. Protein Sci 12:403–411

Marvin DA, Wachtel EJ (1976) Structure and assembly of filamentous bacterial viruses. Philos Trans R Soc Lond Ser B 276:81–98

Marvin DA, Nave C, Ladner JE, Fowler AG, Brown RS, Wachtel EJ (1981) Macromolecular structural transitions in Pf1 filamentous bacterial virus. In: Balaban M, Sussman JL, Traub W, Yonath A (eds) Structural aspects of recognition and assembly in biological macromolecules. Balaban ISS, Rehovot, pp 891–910

Marvin DA, Bryan RK, Nave C (1987) Pf1 *Inovirus*: electron density distribution calculated by a maximum entropy algorithm from native fibre diffraction data to 3 Å resolution and single isomorphous replacement data to 5 Å resolution. J Mol Biol 193:315–343

Marvin DA, Hale RD, Nave C, Helmer-Citterich M (1994) Molecular models and structural comparisons of native and mutant class I filamentous bacteriophages Ff (fd, f1, M13), If1 and IKe. J Mol Biol 235:260–286

Marvin DA, Welsh LC, Symmons MF, Scott WRP, Straus SK (2006) Molecular structure of fd (f1, M13) filamentous bacteriophage refined with respect to X-ray fibre diffraction and solid-state NMR data supports specific models of phage assembly at the bacterial membrane. J Mol Biol 355:294–309

Melo F, Feytmans E (1998) Assessing protein structures with a non-local atomic interaction energy. J Mol Biol 277:1141–1152

Russel M, Model P (2006) Filamentous phage. In: Calendar R (ed) The bacteriophages, 2nd edn. Oxford University Press, USA, pp 146–160

Schwieters CD, Kuszewski JJ, Tjandra N, Clore GM (2003) The Xplor-NIH NMR molecular structure determination package. J Magn Reson 160:65–73

Schwieters CD, Kuszewski JJ, Clore GM (2006) Using Xplor-NIH for NMR molecular structure determination. Prog NMR Spectrosc 48:47–62

Thiriot DS, Nevzorov AA, Zagyanskiy L, Wu CH, Opella SJ (2004) Structure of the coat protein in Pf1 bacteriophage determined by solid-state NMR spectroscopy. J Mol Biol 341:869–879

Tombolato F, Ferrarini A, Grelet E (2006) Chiral nematic phase of suspensions of rodlike viruses: left-handed phase helicity from a right-handed molecular helix. Phys Rev Lett 96:258302(4)

Wang H, Stubbs G (1993) Molecular dynamics in refinement against fiber diffraction data. Acta Crystallog Sect A 49:504–513

Wang J, Denny J, Tian C, Kim S, Mo Y, Kovacs F, Song Z, Nishimura K, Gan Z, Fu R, Quine JR, Cross TA (2000) Imaging membrane protein helical wheels. J Magn Reson 144:162–167

Webster RE (2001) Filamentous phage biology. In: Barbas CF III, Burton DR, Scott JK, Silverman GJ (eds) Phage display: a laboratory manual. Cold Spring Harbor Laboratory Press, Cold Spring Harbor, pp 1.1–1.37

Welsh LC, Symmons MF, Marvin DA (2000) The molecular structure and structural transition of the α-helical capsid in filamentous bacteriophage Pf1. Acta Crystallogr Sect D 56:137–150

Zeri AC, Mesleh MF, Nevzorov AA, Opella SJ (2003) Structure of the coat protein in fd filamentous bacteriophage particles determined by solid-state NMR spectroscopy. Proc Natl Acad Sci USA 100:6458–6463